Codimension-one tangency bifurcations of global Poincaré maps of four-dimensional vector fields

Bernd Krauskopf, Clare M Lee‡ and Hinke M Osinga

Bristol Centre for Applied Nonlinear Mathematics, Department of Engineering Mathematics, University of Bristol, Bristol BS8 1TR, United Kingdom

Abstract.

When one considers a Poincaré return map on a general unbounded $(n-1)$-dimensional section in a vector field in $\mathbb{R}^n$ there are typically points where the flow is tangent to the section. The only notable exception is when the system is (equivalent to) a periodically forced system. The tangencies cause bifurcations of the Poincaré return map when the section is moved when there are no bifurcations in the underlying vector field. The interaction of invariant manifolds and the tangency loci on the surface gives rise to discontinuities of the Poincaré map and there can be open regions where the map is not defined. We study the case of the four-dimensional phase space $\mathbb{R}^4$. Specifically, we make use of tools from singularity theory and flowbox theory to present normal forms of the codimension-one tangency bifurcations in the neighbourhood of a tangency point.

AMS classification scheme numbers: 37C10, 37G05 37G25, 58K50.

1. Introduction

In many applications one is faced with the task of understanding the dynamics of a mathematical model given by a system of ordinary differential equations. Written as an autonomous vector field, such a dynamical system takes the general form

$$\dot{\mathbf{x}} = f(\mathbf{x}, \lambda), \quad \mathbf{x} \in X, \quad \lambda \in \mathbb{R}^m, \tag{1}$$

where X is the phase space, λ is a (vector-valued) parameter, and $f : X \to X$ is sufficiently smooth. In this paper we are interested in the important case that the phase space X is Euclidean and of dimension at most four, that is, $X = \mathbb{R}^n$ for $n \leq 4$. The dynamics is given by the flow Φ associated with (1).

An important tool for analysing the dynamics of a vector field is to consider the dynamics of a Poincaré return map P on a suitable codimension-one section Σ, (i.e. Σ is of dimension $n-1$). The classic application of the Poincaré map is the study of periodic orbits. One chooses a small, local section transverse to a given periodic orbit, then the image of a point $\mathbf{x} \in \Sigma$ under P is given as the next intersection of the orbit

‡ corresponding author; email: Clare.Lee@bristol.ac.uk

of $\mathbf{x}$ with Σ, formally,

$$\begin{aligned} P \;:\; & \Sigma \to \Sigma \\ & \mathbf{x} \mapsto P(\mathbf{x}) := \Phi^{t_{\mathbf{x}}}(\mathbf{x}), \end{aligned} \tag{2}$$

where $t_{\mathbf{x}}$ is the time to the next intersection with Σ. The return map back to the local section is a local diffeomorphism (a smooth map with a smooth inverse) in a neighbourhood of the intersection point of the periodic orbit with the section, which is a fixed point under this Poincaré map. Hence, the stability analysis of the periodic orbit in the full phase space is reduced to the study of the fixed point of the Poincaré map; see standard textbooks such as [7, 9, 19].

Poincaré maps are also used to study other invariant sets, both theoretically and in experiments, for example see [14, 15]. One typically records *all* intersection points, possibly after transients died down, of some orbit with a suitable section (typically some hyperplane). The requirement here is that the orbit actually intersects the section repeatedly. Note that one often records maxima and/or minima of a time series, which is equivalent to considering the intersection points of the derivative of the time series with the section where the value is zero. In other words, one is typically interested in the dynamics on an unbounded or global section, and not only on some small, local neighbourhood.

Except in the case that one considers the stroboscopic map of a periodically forced system, the Poincaré map is *not* a diffeomorphism on the entire global section [22]. Note that P in (2) is well defined at $\mathbf{x}$ only if $0 \leq \inf\{t > 0 \mid \Phi^t(\mathbf{x}) \in \Sigma\} < \infty$. In general there may be points in the section Σ whose trajectories do not return to Σ in either forward or backward time, meaning that the Poincaré map or its inverse is undefined. But even if the Poincaré map is well defined, another issue arises, namely, for a general (non-periodically forced) vector field and any chosen global section Σ, there is a non-empty set of points where the flow is tangent to the section. This set is called the *critical tangency locus*, and it is formally given as

$$C := \{\mathbf{x} \in \Sigma \mid f(\mathbf{x}) \cdot \vec{n}_\Sigma(\mathbf{x}) = 0\}, \tag{3}$$

where $\vec{n}_\Sigma(\mathbf{x})$ is the unit normal to Σ at the point $\mathbf{x}$. Importantly, the Poincaré map, defined as the kth return to Σ (for fixed $k \geq 1$), is discontinuous at any point on the critical tangency locus C. This is because the number of intersections increases or decreases by one at the tangency; [10, 2, 3, 4]. The kth iterate of the global Poincaré map can be extended continuously across C by considering the $(k \pm 1)$st iterate of P in the adjoining region. The choice of the sign follows from the condition that $t_{\mathbf{x}}$, the time to the next intersection, depends continuously on $\mathbf{x}$ across C. We remark that this extension is not unique as it depends on which open region of $\Sigma \setminus C$ one starts in. Furthermore, the continuous extension of P is not differentiable at C, meaning that P cannot be extended across C as a diffeomorphism. What is more, the existence of the set C gives rise to bifurcations of invariant sets in the section Σ that are *not* bifurcations of the underlying vector field itself. Since the Poincaré map is used as a tool to study

the dynamics of the vector field, it is important to classify this type of bifurcation of only the Poincaré map itself.

We are concerned with an important class of such bifurcations, which we refer to as *tangency bifurcations*. A tangency bifurcation is characterised by the tangency of a smooth invariant manifold of a given dimension with the section Σ. It can be brought about by changing either a system parameter or by moving Σ. We studied this type of bifurcation in [10] for vector fields up to dimension $n = 3$, that is, for Poincaré maps on sections of dimension one and two. In this paper we present normal forms for all codimension-one tangency bifurcations of vector fields in $\mathbb{R}^4$. In light of the difficulty of visualising dynamics in four space dimensions, considering a Poincaré map on a three-dimensional section is particularly useful in this case. Hence, the list of tangency bifurcations presented here is of direct use for the interpretation of the dynamics of Poincaré maps on global three-dimensional sections.

Any tangency bifurcation necessarily takes place at some point in the critical tangency locus C, and it can be classified by its order of tangency; see section 2 for details. We consider the situation locally near the tangency point and assume that the respective local piece of the invariant manifold be part of an invariant periodic orbit, invariant torus, or of a stable or unstable manifold.

Specifically, the normal forms of the codimension-one tangency bifurcations are presented in a standard flowbox with parallel flow along one of the axes. A flowbox is simply a domain in phase space that does not contain any compact invariant sets, such as equilibria, is bounded by orbit segments and transverse in- and out-sets of codimension one. Note that it is possible to find a flowbox near any tangency bifurcation which, according to the Flowbox Theorem [13], can be mapped diffeomorphically to the standard flowbox by 'straightening out' the flow. At the moment of tangency bifurcation there is one orbit of (1), which is part of some invariant manifold M, that is tangent to the three-dimensional section precisely at the tangency point associated with the bifurcation. It is the order of this tangency that determines the geometry of the section within the standard flowbox. Note that the critical tangency locus on the three-dimensional section is of dimension two. The order of contact in the directions perpendicular to this orbit determine the geometry of the manifold M inside the flowbox. In fact it suffices to classify the cases when the manifold M is also a codimension-one hypersurface, i.e. of dimension three in a four-dimensional flowbox. The one parameter unfolding of the tangency bifurcation is given by moving the section up and down.

It is very difficult to show the interaction of two three-dimensional hypersurfaces in a four-dimensional flowbox. However, a tangency bifurcation can be characterised and understood by the interaction of the two-dimensional projections of the section and the manifold in the three-dimensional in-set of the flowbox. Namely, the situation in the in-set determines the geometry of the two-dimensional intersection of the manifold with the three-dimensional section. Hence, each codimension-one tangency bifurcation is presented by images that show the flowbox in the in-set and in the section before, at and after the bifurcation. The figures in this paper have been rendered directly from

the respective normal forms.

This paper is organised as follows. In section 2 we introduce some notation as needed to provide background information on tangency bifurcations. There we already provide the list of all codimension-one tangency bifurcations for vector fields of dimension up to four. Section 3 summarises the results from [10] on tangency bifurcations for vector fields of dimension up to three; in particular, we emphasise how the respective manifolds in the in-set determine the situation in the one- or two-dimensional section. The normal forms of the tangency bifurcations for vector fields on $\mathbb{R}^4$ are presented one by one in section 4. Finally, we discuss our results and conclude in section 5.

2. Background and notation

We are interested in how the flow of a vector field on $\mathbb{R}^n$ interacts globally with a Poincaré section Σ. By this we mean that Σ is a smooth manifold of dimension $n-1$ that is unbounded in all directions. In other words, Σ divides the phase space $\mathbb{R}^n$ into two disjoint parts. The notion of a global section is quite natural, and the easiest and often used example is that Σ is an $(n-1)$-dimensional hyperplane.

We consider here the general case of a system that is not periodically forced. Hence, the critical tangency locus C defined in (5) is nonempty [22]. At a regular point in C the flow makes a quadratic tangency with the section Σ. It follows from the Implicit Function Theorem that C consists generically of smooth codimension-one submanifolds of Σ. The codimension-one submanifolds of C that correspond to regular points meet in submanifolds of higher codimension, which correspond to higher-order tangencies. To be specific, for $n = 2$ the set C consists generically of isolated points in the one-dimensional section Σ. For $n = 3$ the critical tangency locus consists generically of smooth one-dimensional curves of regular points in the two-dimensional section Σ that meet at isolated cusp points, where the flow has a cubic tangency with the section Σ. For the case $n = 4$, which is the main subject here, C consists generically of smooth two-dimensional surfaces in the three-dimensional section Σ. Two surfaces meet along a one-dimensional curve of cusp points. On the curve of cusp points one may find isolated points where the flow has a quartic tangency (i.e., of order four) with Σ; such a point is also known as a swallowtail point.

Overall, the critical tangency locus C divides the section Σ into open regions. Neighbouring regions (divided by regular points of C) correspond to different directions of the flow, with respect to the normal to Σ. Note that Σ is orientable, so that its unit normal $\vec{n}_\Sigma(\mathbf{x})$ can be 'transported' unambiguously along Σ by moving the point $\mathbf{x}$.

2.1. Classification of tangency bifurcations

Our interest is in how a smooth invariant manifold M, of dimension ℓ composed of a family of orbits of vector field (1), interacts with a Poincaré section Σ. In order

to introduce our notion of bifurcation, we first recall from [10] the relevant notion of topological equivalence.

Definition 1. *Consider two open neighbourhoods U_1 and U_2 of $\mathbb{R}^n$. Suppose that $\Sigma_1 \subset U_1$ and $\Sigma_2 \subset U_2$ are $(n-1)$-dimensional smooth sections that divide U_1 and U_2 into two parts and have critical tangency loci C_1 and C_2, respectively. Suppose further, that there is an ℓ-dimensional invariant manifold $M_1 \subset U_1$, and an ℓ-dimensional invariant manifold $M_2 \subset U_2$.*
We say that the flow Φ_1 on U_1 is Σ-M-topologically equivalent *to the flow Φ_2 on U_2 if there exists a homeomorphism $h : U_1 \to U_2$ such that*

(E1) h maps orbits of Φ_1 in U_1 to orbits of Φ_2 in U_2 and respects the direction of time;

(E2) h maps Σ_1 to Σ_2 and C_1 to C_2;

(E3) h maps M_1 to M_2.

Note that (E2) and (E3) ensure that $h|_{\Sigma_1}$ maps $M_1 \cap \Sigma_1$ to $M_2 \cap \Sigma_2$. The notion of topological equivalence in Definition 1 implies notions of structural stability. Namely, a phase portrait (a particular arrangement of Σ, C and M) is structurally stable if all sufficiently small (and smooth) perturbations are topologically equivalent. At a bifurcation point the phase portrait is not structurally stable.

In this paper we study bifurcations that are not bifurcations of the underlying flow, yet change the topological structure of the invariant objects of the Poincaré map on the section Σ. That is, we consider the case that there is a homeomorphism h that satisfies (E1) and (E2), but not (E3). To be even more specific, we exclude the case that an equilibrium crosses Σ. Instead consider the case of a tangency bifurcation of an ℓ-dimensional smooth invariant manifold M of vector field (1). A tangency bifurcation arises when an orbit

$$\mathcal{O}(\mathbf{x}^*) = \{\Phi^t(\mathbf{x}^*) \mid t \in \mathbb{R}\}. \tag{4}$$

is tangent to the given $(n-1)$-dimensional Poincaré section Σ at a point $\mathbf{x}^* \in M \cap \Sigma$. Note that a manifold M of dimension one consists of a single orbit. However, for $\ell \geq 2$ the manifold M consists of a smooth $(\ell-1)$-dimensional family of orbits. Therefore, to classify the tangency bifurcation we need to take into account both the order of the tangency of the orbit $\mathcal{O}(\mathbf{x}^*)$ as well as the nature of the tangency between M and Σ in the family direction of M, which is transversal to the direction of the flow. Following [10], we use the classification of tangency bifurcations, which is based on the intersection of the tangent spaces $T_M(\mathbf{x}^*)$ and $T_\Sigma(\mathbf{x}^*)$.

Definition 2. *Let M be an ℓ-dimensional invariant manifold of a vector field f on $\mathbb{R}^n$ with a given $(n-1)$-dimensional global section Σ. Suppose that the following conditions are satisfied:*

(B1) there is a point $\mathbf{x}^* \in M \cap \Sigma$ such that the orbit $\mathcal{O}(\mathbf{x}^*)$ has a tangency of degree $d \in \mathbb{N}$ with Σ at $\mathbf{x}^*$, where we assume that the tangency is at least quadratic, that is, $d \geq 2$;

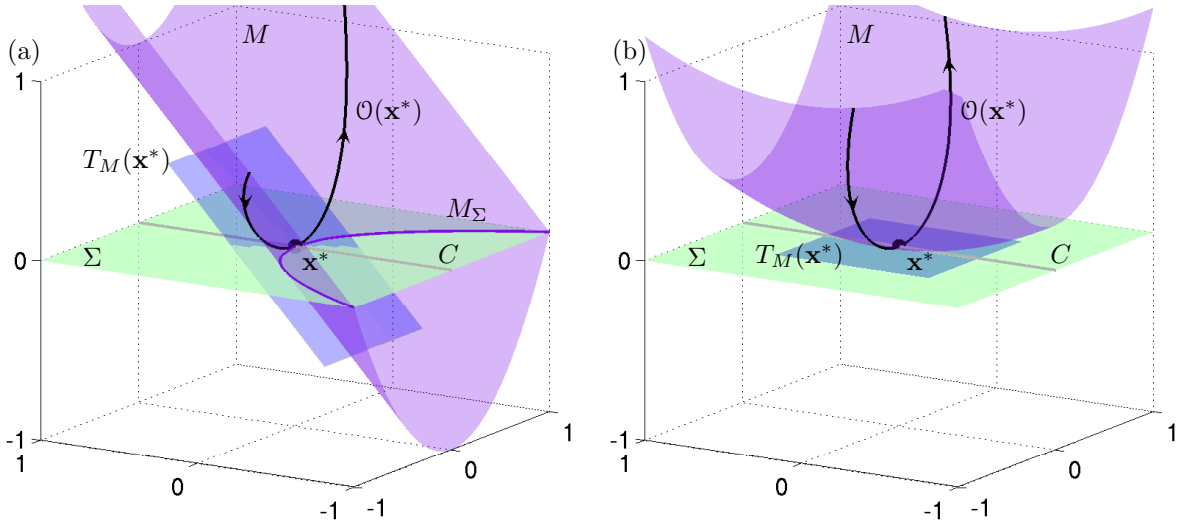

Figure 1. Two cases where an orbit $\mathcal{O}(\mathbf{x}^*)$ on a two-dimensional manifold M (purple) has a quadratic tangency with a planar section Σ (green). The situation in panel (a) is structurally stable, while that in panel (b) is of codimension one; which case occurs is determined by the dimension of the intersection of the tangent space $T_M(\mathbf{x}^*)$ of M (blue) with the tangent space $T_\Sigma(\mathbf{x}^*) = \Sigma$.

(B2) The dimension of the orthogonal complement N of $f(\mathbf{x}^*)$ in $T_M(\mathbf{x}^*) \cap T_\Sigma(\mathbf{x}^*)$ is p; and

(B3) The point $\mathbf{x}^*$ is a critical point of codimension q of the restriction $\vartheta|_N$ to N of the local chart $\vartheta : T_M(\mathbf{x}^*) \to \mathbb{R}^n$ of the manifold M at $\mathbf{x}^*$.

Then we say that M and Σ have a d-tangency with singularity dimension p and singularity codimension q *at $\mathbf{x}^*$ (or d-p-q-tangency or short).*

To clarify Definition 2, figure 1 shows two examples of tangency bifurcations of vector fields in $\mathbb{R}^3$. In both panels (a) and (b) a two-dimensional invariant manifold M (purple) has an orbit $\mathcal{O}(\mathbf{x}^*)$ that has a quadratic tangency with a two-dimensional planar Poincaré section Σ (green). This quadratic tangency takes place at a regular point $\mathbf{x}^*$ of the critical tangency locus C. The difference between the two cases is the following. In figure 1(a) the manifold M is not tangent to Σ in the family direction, which means that the tangent space $T_M(\mathbf{x}^*)$ (blue) of M at $\mathbf{x}^*$ intersects $T_\Sigma(\mathbf{x}^*) = \Sigma$ in a one-dimensional line, which is the tangent $f(\mathbf{x}^*)$ to the orbit $\mathcal{O}(\mathbf{x}^*)$ at $\mathbf{x}^*$. Hence, this is a structurally stable codimension-zero situation. As figure 1(a) shows, when the section (or the manifold) is moved up or down we still find a unique point in $\Sigma \cap M$ with the same properties as $\mathbf{x}^*$. If M were to be a one-dimensional manifold that only contains the orbit $\mathcal{O}(\mathbf{x}^*)$ then this would be a 2-0-0 tangency, which is of codimension-one. By contrast, in figure 1(b) the tangent spaces $T_M(\mathbf{x}^*)$ and $T_\Sigma(\mathbf{x}^*)$ coincide, so that their intersection is two-dimensional. This means that the manifold has a second direction of tangency, apart from the direction $f(\mathbf{x}^*)$ of the flow. We are dealing with a 2-1-1 tangency according to Definition 2. In particular, $p = 1$ because the manifold

is tangent to Σ in N, which in turn means that $\mathbf{x}^*$ is indeed a critical point of $\vartheta|_N$ in (B3). Since the tangency with respect to the one-dimensional orthogonal complement N is quadratic, the codimension of this critical point is $q = 1$. Notice that the situation in figure 1(b) is no longer structurally stable. Instead, the 2-1-1 tangency in $\mathbb{R}^3$ is of codimension one. It can be unfolded by moving either the section or the manifold up and down.

The notion of codimension can be formulated for any d-p-q-tangency of an ℓ-dimensional manifold with a Poincaré section of a vector field f on $\mathbb{R}^n$. We have the following result.

Proposition 1. *A d-p-q-tangency of an ℓ-dimensional invariant manifold $M \subset \mathbb{R}^n$ with a global section Σ is of codimension one if $\ell = d + q - 1$, where $p < \ell < n$.*

This proposition is a special case of the general formula for codimension given in [10]. Notice that the codimension does not depend on the dimension n of the phase space. Therefore, it is most convenient to study a given d-p-q-tangency in the smallest possible phase space, which is that of dimension $n = \ell + 1$. In other words, it is possible to list the codimension-one tangency bifurcations by the dimension n of the phase space, where one only needs to consider a manifold of dimension $\ell = n - 1$. Hence, the question is how the two $(n-1)$-dimensional smooth manifolds M and Σ interact near a tangency point $\mathbf{x}^* \in C$. This gives rise to the following classification of codimension-one tangency bifurcations for $n \leq 4$.

In $\mathbb{R}^2$ for a manifold M of dimension $\ell = 1$:

(T1). the 2-0-0-tangency: a quadratic tangency of the orbit that defines M; the unfolding is presented in section 3.1.

In $\mathbb{R}^3$ for a manifold M of dimension $\ell = 2$:

(T2). the 2-1-1-tangency: a quadratic tangency of an orbit on M and a quadratic tangency with respect to the one-dimensional space N. There are two cases, depending on the relative directions of the two quadratic tangencies; the unfoldings are presented in section 3.2.

(T3). 3-0-0-tangency for $\ell = 2$: a cubic tangency of an orbit on M; the unfolding is presented in section 3.3.

In $\mathbb{R}^4$ for a manifold M of dimension $\ell = 3$:

(T4). the 2-2-2-tangency: a quadratic tangency of an orbit on M with quadratic tangencies in the two additional tangent directions that span the two-dimensional space N. There are two cases, depending on the relative directions of the quadratic tangencies; the unfoldings are presented in section 4.1.

(T5). the 2-1-2-tangency: a quadratic tangency of an orbit on M that makes a cubic tangency with respect to the one-dimensional space N; the unfoldings are presented in section 4.2.

(T6). the 3-1-1-tangency: a cubic tangency of an orbit on M that makes a quadratic tangency with respect to the one-dimensional space N. There are two cases, depending on the relative directions of the cusp and the quadratic tangency; the unfoldings are presented in section 4.3.

(T7). 4-0-0-tangency for $\ell = 3$: A quartic tangency of an orbit on M; the unfolding is presented in section 4.4.

2.2. Normal form setting in standard flowbox

A codimension-one tangency bifurcation can be unfolded by changing a single system parameter to alter the position of the manifold M. Alternatively, one can keep the vector field fixed and change the position of the section. While the first option appears to be the more natural one in many applications, changing only the section gives topologically equivalent unfoldings. This second option is used here as the more convenient choice to define normal forms of the codimension-one tangency bifurcations.

We consider from now on a one-parameter family of global sections Σ_s, where the dependence on the parameter s is smooth. Each of these sections has a critical tangency locus $C = C(s)$ that depends on s. To help us understand the geometry of the flow we introduce another geometrical object: the *extended critical locus* $\mathcal{C}$, defined as

$$\mathcal{C} = \bigcup_s C(s). \tag{5}$$

Since the dependence of Σ_s on s is smooth, $\mathcal{C}$ is a smooth codimension-one submanifold of the phase space $\mathbb{R}^n$. Hence, its dimension is $n-1$, the same as that of the section Σ_s and the manifold M. Generically, the extended critical locus is transverse to Σ_s. Therefore, knowing properties of the flow through $\mathcal{C}$ gives new geometric insight. We introduce the critical tangency locus D on $\mathcal{C}$, which is given by

$$D := \{\mathbf{x} \in \mathcal{C} \mid f(\mathbf{x}) \cdot \vec{n}_{\mathcal{C}}(\mathbf{x}) = 0\}, \tag{6}$$

where $\vec{n}_{\mathcal{C}}(\mathbf{x})$ is the unit normal to $\mathcal{C}$ at the point $\mathbf{x}$. As with C on Σ the tangency locus D in $\mathcal{C}$ generically consists of codimension-one submanifolds that divide $\mathcal{C}$ into regions with opposite directions of the flow relative to the normal bundle of $\mathcal{C}$.

Because a tangency bifurcation does not involve equilibria in Σ, it is possible to consider the phase portrait in a flowbox near the point $\mathbf{x}^* \in C$ at which the tangency takes place. This flowbox is given by an in-set and an out-set transverse to the flow, which are connected by orbit segments. According to the Flowbox Theorem [13] any flowbox can be mapped diffeomorphically to a standard flowbox in $\mathbb{R}^n$, which we define here as

$$\begin{cases} \dot{u} &= 1, \\ \dot{v} &= 0, \end{cases} \tag{7}$$

where $u \in [-1,1]$ and $v \in [-1,1]^{n-1}$. It follows that the in-set and the out-set of the standard flowbox are

$$I = \{u = -1\} \quad \text{and} \quad O = \{u = +1\}. \tag{8}$$

To realise a *d*-*p*-*q*-tangency bifurcation in the standard flowbox given by (7), one needs to provide formulae for the family of sections Σ_s and the manifold M. More specifically, for any s the section Σ_s is a hypersurface whose geometry is determined by the order d of the tangency of the orbit $\mathcal{O}(\mathbf{x}^*)$. The manifold M in the flowbox is also a hypersurface, but its geometry determines the nature of the tangency in the other directions (with respect to the space N of Definition 2), as encoded by p and q. Our approach of constructing normal forms is in the spirit of singularity theory [5], which suggests how the respective surfaces should be chosen. However, one also has to deal with the flow in the flowbox. The situation is very similar to the one encountered when one considers flows on phase spaces with boundaries [18, 20, 16] or when studying piecewise-smooth vector fields [21]. As explained in [10], transformations can be constructed (while observing the restrictions imposed by the presence of the flow) that allow one to bring a given tangency bifurcation into its normal form in the standard flowbox; see also [18, 11].

In our approach the family Σ_s is a standard singularity surface given by the tangency-order d that moves in the v_{n-1}-direction with the parameter s. For the list in section 2.1 we need to consider the three cases for $d = 2$, 3 and 4, which give rise to fold, cusp and swallowtail surfaces, respectively; compare, for example, [17, section 9.4]. From the definition of Σ_s one immediately obtains formulae for the critical tangent locus C, the extended critical locus $\mathcal{C}$ and its critical tangency locus D.

Our family of (quadratic) fold surfaces in $\mathbb{R}^n$ for $n \geq 2$ is given by

$$\begin{aligned}
\Sigma_s &= \{(u, v_1, \ldots, v_{n-1}) \in \mathbb{R}^n \mid v_{n-1} - u^2 - s = 0\}, && (9)\\
C(s) &= \{(u, v_1, \ldots, v_{n-1}) \in \Sigma_s \mid u = 0 \ \text{ and } \ v_{n-1} = s\}, && (10)\\
\mathcal{C} &= \{(u, v_1, \ldots, v_{n-1}) \in \mathbb{R}^n \mid u = 0\}, && (11)\\
D &= \emptyset. && (12)
\end{aligned}$$

Our family of (cubic) cusp surfaces in $\mathbb{R}^n$ for $n \geq 3$ is given by

$$\begin{aligned}
\Sigma_s &= \{(u, v_1, \ldots, v_{n-1}) \in \mathbb{R}^n \mid v_1\, u - u^3 + v_{n-1} - s = 0\}, && (13)\\
C(s) &= \{(u, v_1, \ldots, v_{n-1}) \in \Sigma_s \mid v_1 = 3u^2,\ v_{n-1} = s - 2u^3\}, && (14)\\
\mathcal{C} &= \{(u, v_1, \ldots, v_{n-1}) \in \mathbb{R}^4 \mid v_1 = 3u^2\}, && (15)\\
D &= \{(u, v_1, \ldots, v_{n-1}) \in \mathcal{C} \mid u = 0,\ v_1 = 0\}. && (16)
\end{aligned}$$

Our family of (quartic) swallowtail surfaces in $\mathbb{R}^n$ for $n \geq 4$ is given by

$$\begin{aligned}
\Sigma_s &= \{(u, v_1, \ldots, v_{n-1}) \in \mathbb{R}^n \mid v_{n-1} + v_2 u + v_1 u^2 + u^4 - s = 0\}, && (17)\\
C(s) &= \{(u, v_1, \ldots, v_{n-1}) \in \Sigma_s \mid v_2 = -2v_1 u - 4u^3,\\
&\qquad\qquad v_{n-1} = v_1 u^2 + 3u^4 + s\}, && (18)\\
\mathcal{C} &= \{(u, v_1, \ldots, v_{n-1}) \in \mathbb{R}^n \mid v_2 = -2v_1 u - 4u^3\}, && (19)\\
D &= \{(u, v_1, \ldots, v_{n-1}) \in \mathcal{C} \mid v_1 = -6u^2,\ v_2 = 8u^3\}. && (20)
\end{aligned}$$

Now that families Σ_s have been determined for the different cases of tangency, the task is to define manifolds M that represent the different tangencies in the additional

directions. Note that we have chosen to define the section using v_{n-1} and the lowest v_i coordinates. This means that an increase in the dimension only changes Σ_s to the extent that a new coordinate is added. As a result, the manifolds that are defined in I are also defined in terms of v_{n-1} and the lowest v_i-coordinates with all other v_i being set to zero. Importantly the geometry of the manifolds on the in-set of the standard flowbox determines the invariant set $M \cap \Sigma$ in the Poincaré section, for any given tangency bifurcation. In the next section we present the tangency bifurcations (T1)–(T3) for $n = 2$ and $n = 3$ from [10] from this point of view. Section 4 then presents the tangency bifurcations (T4)–(T7) for $n = 4$.

Our images of unfoldings in the next sections are necessarily increasing in complication. To help their interpretation we use a single colour code throughout for the different objects (and their projections): the manifold M is purple, the section Σ_s is green, the critical tangency locus C and the extended critical tangency locus $\mathcal{C}$ are grey, and the critical tangency locus D is white. The projection $\widehat{C}$ of C onto the in-set divides I into regions. Orbits originating in one such region have the same number of intersections with Σ_s before exiting the flowbox. In our figures each region of I whose orbits intersect Σ_s at least once is shown in green; furthermore, the number of intersections is indicated by circled numbers ①–④. A region of I whose orbits do not intersect Σ_s at all is white.

Furthermore, we indicate the direction of the flow on $\Sigma \setminus C$ and on $\mathcal{C} \setminus D$ as follows. The normal $\vec{n}_\Sigma(\mathbf{0})$ to Σ at the tangency point $\mathbf{x}^* = \mathbf{0}$ always lies in the v_{n-1}-direction, and we choose $\vec{n}_\Sigma(\mathbf{0})$ such that it points in the direction of positive v_{n-1}. Furthermore, we choose the normal $\vec{n}_\mathcal{C}(\mathbf{0})$ to $\mathcal{C}$ such that $\vec{n}_\Sigma(\mathbf{0})$, $n_\mathcal{C}(\mathbf{0})$ and $f(\mathbf{0})$ form a right-handed coordinate system. The direction of the normals $\vec{n}_\Sigma(\mathbf{x})$ and $\vec{n}_\mathcal{C}(\mathbf{x})$ at some general point $\mathbf{x}$ of Σ_s or $\mathcal{C}$, respectively, is then obtained by the condition that it agrees with that of $\vec{n}_\Sigma(\mathbf{0})$ and $\vec{n}_\mathcal{C}(\mathbf{0})$ when it is moved to $\mathbf{0}$ along the surface (which is orientable). In all dimensions and for all degrees of tangency, we denote a region of $\Sigma_s \setminus C$ with the symbol $\odot$ when the flow is such that $f(\mathbf{x}) \cdot \vec{n}_\Sigma(\mathbf{x}) > 0$, and with the symbol $\otimes$ otherwise. Similarly, regions of $\mathcal{C} \setminus D$ are denoted with the symbols $\odot$ and $\otimes$, depending on whether $f(\mathbf{x}) \cdot \vec{n}_\mathcal{C}(\mathbf{x}) > 0$ or not. The direction of the flow is readily determined for the three different cases of sections from formulae (9)–(17).

3. Tangency bifurcations in dimensions one and two

The tangency bifurcations (T1)–(T3) for $n = 2$ and $n = 3$ from section 2.1 were the topic of [10]. They are presented here for completeness, but also to help with the interpretation of the tangency bifurcations for $n = 4$ in the next section. Moreover, the presentation differs slightly from that in [10] in that the emphasis is now on how the projections of the section and the manifold in the in-set of the standard flowbox determine the invariant set $M_\Sigma = M \cap \Sigma_s$.

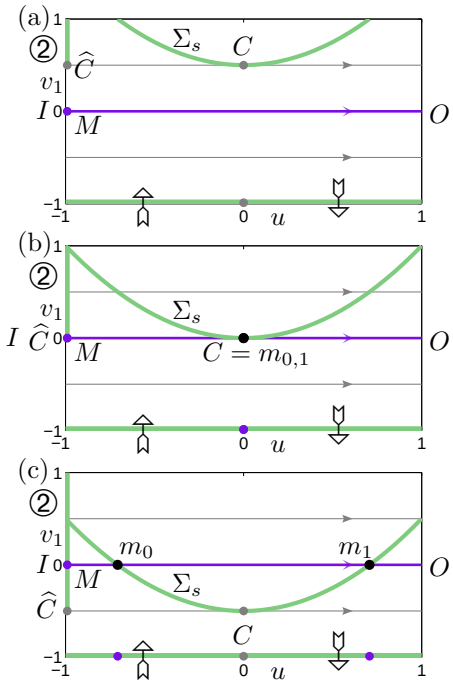

Figure 2. The unfolding of the 2-0-0 tangency bifurcation of a one-dimensional invariant manifold M (purple) with a global section (green) in the standard flowbox for $n = 2$. Also shown are the projections onto both the in-set I (left boundary of the panels) and the section Σ_s (bottom of the panels); from (a)–(c), $s = 0.5$, $s = 0$, and $s = -0.5$.

3.1. The 2-0-0 tangency bifurcation in $\mathbb{R}^2$

The first codimension-one tangency bifurcation is a quadratic tangency of a single orbit segment on a one-dimensional manifold. As is discussed in [10], the 'classic case' is that the piece of manifold in the flowbox is part of a periodic orbit. It has been observed that this quadratic tangency may give rise to additional branches in a bifurcation diagram when a periodic orbit changes shape with parameter variation [6, 8]. Similarly, when maxima of a time series are recorded, a new maximum arises at an inflection point of the time series, that is, at a tangency bifurcation of the derivative of the time series [12]. The 2-0-0 tangency bifurcation of a one-dimensional manifold is of codimension one for any n.

Proposition 2. *A 2-0-0 tangency of a one-dimensional manifold in* $\mathbb{R}^n$ *is given in the standard flowbox (7) by the family (9) of quadratic sections* Σ_s *with the manifold*

$$M = \{(u, v_1, \ldots, v_{n-1}) \in \mathbb{R}^n \mid v_i = 0 \text{ for } i = 1, \ldots, n-1\}. \tag{21}$$

The normal form is given by $n = 2$.

The unfolding of the 2-0-0 tangency is illustrated in figure 2 with three panels of the standard flowbox for $n = 2$ before, at and after the bifurcation. The critical tangency locus C on the quadratic section Σ_s is at $u = 0$. As s is changed, Σ_s moves down and through the fixed manifold M. For $s = 0$ the two curves Σ_s and M are tangent.

As we explain now, this unfolding can be understood by observing only the situations in the in-set I and in the section Σ_s. The in-set I can be identified with the v_1-space, and it is shown on the left boundaries of the flowbox panels in figure 2. The projection of Σ_s onto I is shown as the green segment where each orbit intersects Σ_s twice. It is bounded by the projection $\widehat{C}$ (grey dot) of the critical tangency locus C onto I, which is the point $v_1 = s$. The manifold M is uniquely determined by $M \cap I$, which is the point $v_1 = 0$ (purple dot). When s is changed, the projection of Σ_s onto I changes because $\widehat{C}$ moves relative to M. As a result, the invariant set $M_\Sigma = M \cap \Sigma_s$ changes within Σ_s. Since Σ_s is a function over the variable u, it can be identified with the u-axis as illustrated at the bottom boundaries of the flowbox panels in figure 2. To the left of C the flow points upward through the section Σ_s and to the right of C it points downward. This is denoted with the symbols $\Uparrow$ and $\Downarrow$ respectively. This choice of symbol is more intuitive in the one-dimensional context than the symbols $\odot$ and $\otimes$.

Figure 2 illustrates that the situation in I indeed determines the situation in Σ_s. Specifically, in panel (a) $s > 0$ so that $M \cap I$ is below $\widehat{C}$ and not in the green region of I, meaning that M does not intersect Σ_s and the set M_Σ is empty. Panel (b) shows the moment of bifurcation when $s = 0$ so that $M \cap I = \widehat{C}$; hence, M is tangent to Σ_s and the set M_Σ consists of a single point (purple dot). Finally, in panel (c) $s < 0$ so that $M \cap I$ is above $\widehat{C}$ and, hence, in the green region of two intersections; as a result, M_Σ consists of two points (purple dots).

3.2. The 2-1-1 tangency bifurcations in $\mathbb{R}^3$

The 2-1-1 tangency bifurcation is the first example of a quadratic tangency bifurcation that occurs in vector fields with phase space of dimension at least three.

Proposition 3. *A 2-1-1 tangency bifurcation of a two-dimensional manifold in* $\mathbb{R}^n$ *is given in the standard flowbox (7) by the family (9) of quadratic sections* Σ_s *with the manifold*

$$M = \{(u, v_1, \ldots, v_{n-1}) \in \mathbb{R}^n \mid v_{n-1} = \pm v_1^2 \,;\; v_i = 0 \text{ for all other } i\,\}. \tag{22}$$

The minus-sign in (22) is referred to as the minimax case and the plus-sign as the saddle case of the 2-1-1 tangency bifurcation. The normal form is given by $n = 3$.

As with the normal form of the 2-0-0 tangency bifurcation for $n = 2$, we can describe the unfolding of the 2-1-1 tangency bifurcation for $n = 3$ by considering only the in-set I and the section Σ_s, which can again be identified (by projection) with the (u, v_1)-plane. Figures 3 and 4 show the minimax case and the saddle case, respectively, on the level of the in-set I (left column) and the section Σ_s (right column), rather than the entire flowbox. The three rows show the phase portraits before, at and after the bifurcation. Note that we consider in Proposition 3 a curved manifold M on the in-set I to represent the tangency in the N-direction perpendicular to the flow. This representation differs from, but is equivalent to that of figures 9 and 10 in [10], where M is represented as a plane. Specifically, the in-set is now given by the (v_1, v_2)-plane, and both cases are

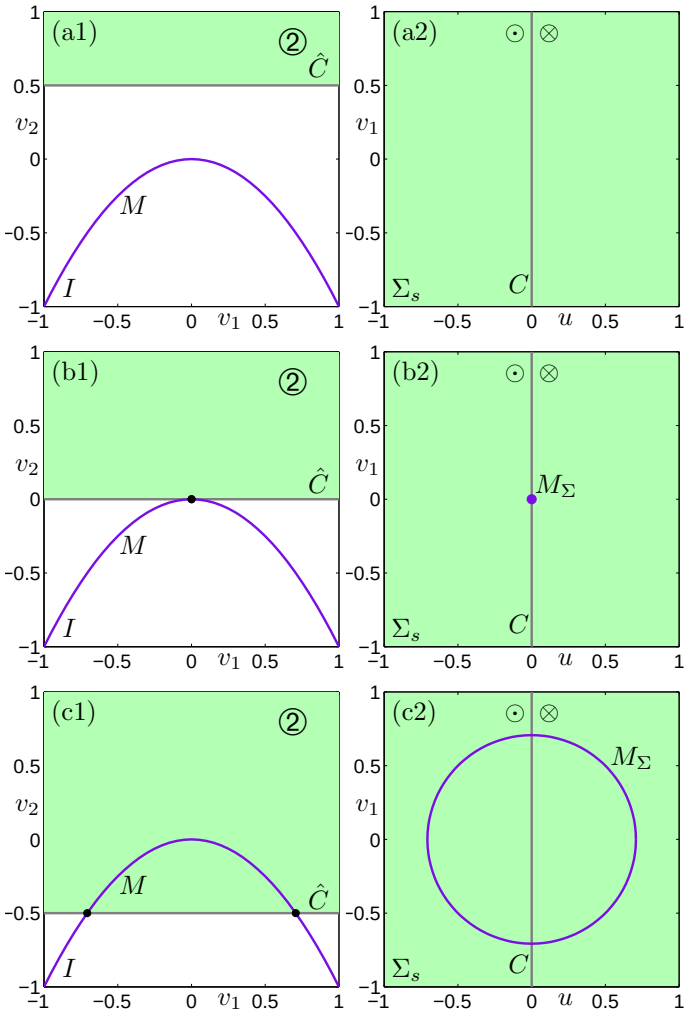

Figure 3. Unfolding of the minimax case of the 2-1-1 tangency bifurcation of a two-dimensional invariant manifold M (purple) with a global section (green); shown are the in-set I (left column) and the section Σ_s (right column); from (a)–(c), $s = 0.5$, $s = 0$, and $s = -0.5$.

characterised by a quadratic tangency between M and $\widehat{C}$ in I. As the panels in the left columns of figures 3 and 4 show, the difference between the two minimax and saddle cases lies in the direction of the curvature of $M \cap I$ in relation to $\widehat{C}$ and the projection of Σ_s. Both figures again illustrate that the situation in I determines the situation in Σ_s.

For the minimax case in figures 3, $M \cap I$ curves away from $\widehat{C}$ and only enters the projection of Σ_s for $s \leq 0$. This means that the set M_Σ is created (or destroyed) in the form of a topological circle. In row (a), $s > 0$ so M does not intersect $\widehat{C}$ or the projection of Σ_s in I, which is why M_Σ is empty. Decreasing s to the bifurcation point for $s = 0$ in row (b), $M \cap I$ becomes tangent to $\widehat{C}$ at a single point, meaning that M_Σ consists of a single point (purple dot). Finally, in row (c), $s < 0$ so $M \cap I$ enters the projection of Σ_s in I and, hence, the set M_Σ is a circle.

For the saddle case in figures 4, $M \cap I$ curves towards $\widehat{C}$ and, therefore, enters the

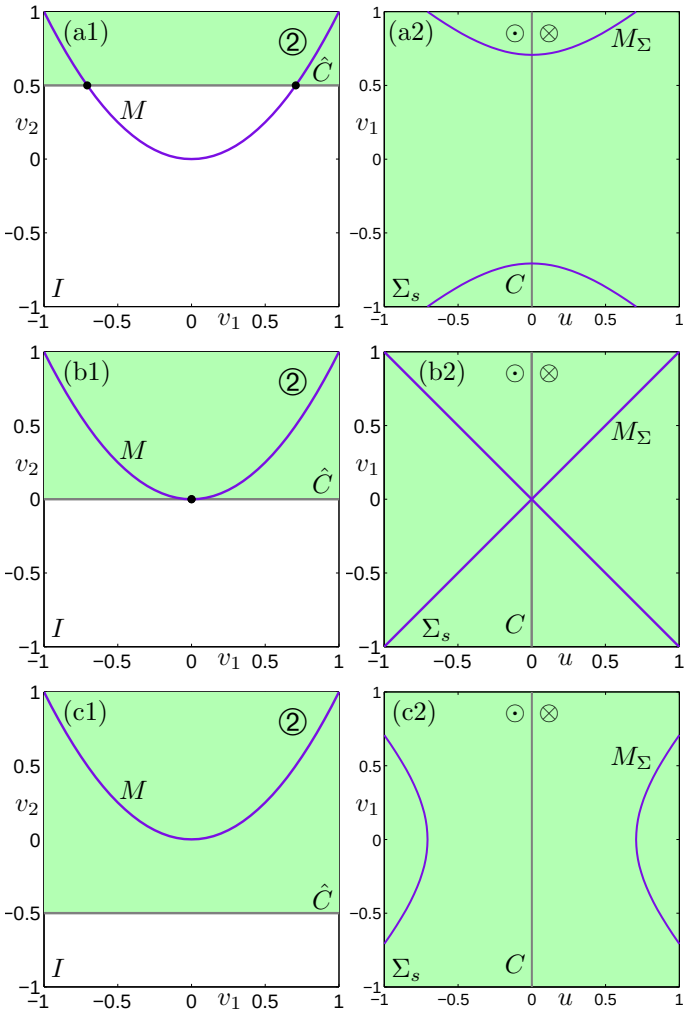

Figure 4. Unfolding of the saddle case of the 2-1-1 tangency bifurcation of a two-dimensional invariant manifold M (purple) with a global section (green); shown are the in-set I (left column) and the section Σ_s (right column); from (a)–(c), $s = 0.5$, $s = 0$, and $s = -0.5$.

projection of Σ_s for all s. Hence, $M_\Sigma \neq \emptyset$ for all s since $M \cap I$ intersects the projection of Σ_s on I for all s. The intersection of M with Σ_s in row (a) consists of two arcs that both cross C, each corresponding to one of two parts of $M \cap I$ inside the projection of Σ_s onto I. At the moment of bifurcation in row (b), $M \cap I$ is totally contained in the projection of Σ_s but is tangent to $\widehat{C}$. This means that the two arcs of M_Σ meet on C to form a cross. For $s < 0$ in row (c), $M \cap I$ is still totally contained in the projection of Σ_s but no longer intersects $\widehat{C}$. Therefore, M_Σ again consists of two arcs but they do not intersect C.

3.3. The 3-0-0 tangency bifurcation in $\mathbb{R}^3$

The 3-0-0 tangency bifurcation is the first tangency bifurcation that involves a cubic tangency of an orbit on the manifold.

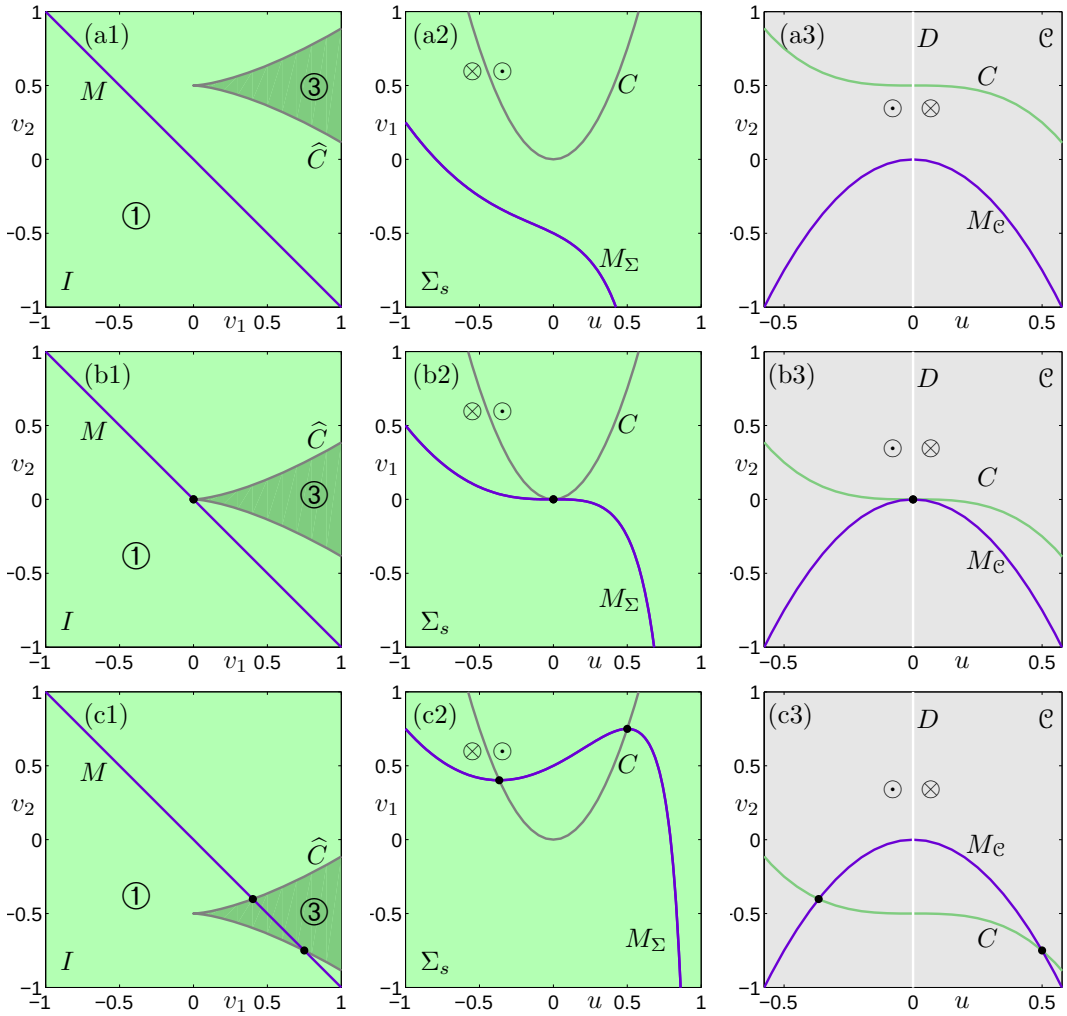

Figure 5. Unfolding of the 3-0-0 tangency bifurcation of a two-dimensional invariant manifold M (purple) with a global section (green); shown are the in-set I (left column), the section Σ_s (middle column) and the extended critical locus $\mathcal{C}$ (right column); from (a)–(c), $s = 0.5$, $s = 0$, and $s = -0.5$.

Proposition 4. *A 3-0-0 tangency bifurcation of a two-dimensional manifold in $\mathbb{R}^n$ is given in the standard flowbox (7) by the family (13) of cubic sections Σ_s with the manifold*

$$M = \{(u, v_1, \ldots, v_{n-1}) \in \mathbb{R}^n \mid v_{n-1} = -v_1\,;\ v_i = 0,\ \text{for all other } i\,\}. \tag{23}$$

The normal form is given by $n = 3$.

Note that the manifold M in Proposition 4 is chosen to be in general position with respect to Σ_s, which reflects the fact that $p = 0$. In particular, M cannot be parallel to either the v_{n-1}- or the v_{n-2}-direction; see [10]. As before, we consider in figure 5 the unfolding of this bifurcation by showing the in-set I and the section Σ_s, which can again be identified (by projection) with the (u, v_1)-plane. For the first time the extended tangency locus $\mathcal{C}$ is nontrivial: it is the parabolic cylinder given by (15) that is divided by the curve D of (16) into two parts with different flow directions. To help with the

understanding of the 3-0-0 tangency bifurcation we also show in figure 5 the situation in $\mathcal{C}$, which can be identified (by projection) with the (u, v_2)-plane.

The 3-0-0 tangency bifurcation for $n = 3$ is shown in figure 5 before, at and after the bifurcation. The critical tangency locus divides Σ_s into two regions of different directions of the flow. Due to the cubic shape of Σ_s, the in-set I is divided by the projection $\widehat{C}$ into two regions ① and ③ where orbits intersect Σ_s once or three times, respectively. Notice the cusp in the curve $\widehat{C}$. As s changes, $\widehat{C}$ and the region of three intersections with Σ_s move and interact with the manifold M. Figure 5 illustrates that the situation in I determines not only the situation in Σ, but also that in $\mathcal{C}$. In row (a) for $s > 0$, $M \cap I$ does not intersect $\widehat{C}$ in panel (a1), meaning that all orbits starting on $M \cap I$ only intersect Σ once within the flowbox. Indeed M_Σ does not intersect C in panel (a2) and the intersection of $C = \mathcal{C} \cap \Sigma$ in $\mathcal{C}$ is above $M_\mathcal{C}$ in panel (a3). At the moment of bifurcation for $s = 0$ in row (b), $M \cap I$ intersects $\widehat{C}$ exactly once at the cusp point; see panel (b1). As a result, Σ_s becomes tangent to M in panel (b2), which can also be seen in $\mathcal{C}$ in panel (b3). Notice that the cubic tangency of M and Σ_s corresponds to a quadratic tangency of M_Σ and C in Σ_0, and of $M_\mathcal{C}$ and C in $\mathcal{C}$. Indeed, the cubic tangency can only take place at the intersection with C and D. For $s < 0$, as in row (c), $M \cap I$ enters the region of I where orbits intersect the section three times within the flowbox. Specifically, the segment of M_Σ with $v_1 > 0$ to the left of C is mapped to Σ_s inside the parabola C, which in turn is mapped to the right of C before exiting the flowbox.

4. Tangency bifurcation in dimension four

We now present all codimension-one tangency bifurcations that appear for the first time in vector fields of dimension at least four; these are cases (T4)–(T7) in the list in section 2. According to Proposition 1, they involve the interaction of a three-dimensional manifold M with a three-dimensional section Σ inside the standard flowbox of dimension four. Since it is practically impossible to visualise this in four dimensions we present the respective unfoldings on the level of the in-set I, the section Σ_s and the extended critical tangency locus $\mathcal{C}$, as was done in section 3. Now all images show spaces of dimension three.

4.1. The 2-2-2 tangency bifurcation in $\mathbb{R}^4$

As our first tangency bifurcation in four dimensions we consider a quadratic tangency of the flow where the tangent spaces of M and Σ_s coincide. Hence, there are two further directions along which the manifold and the section have a quadratic tangency, so that M is given by a quadratic surface in the in-set. As was the case with the 2-1-1 tangency bifurcation of a two-dimensional manifold, there are two different cases depending on the relative directions of the corresponding quadratic curves: either they are all on the same side of Σ_s, or one of them is on one side and the other two are on the side.

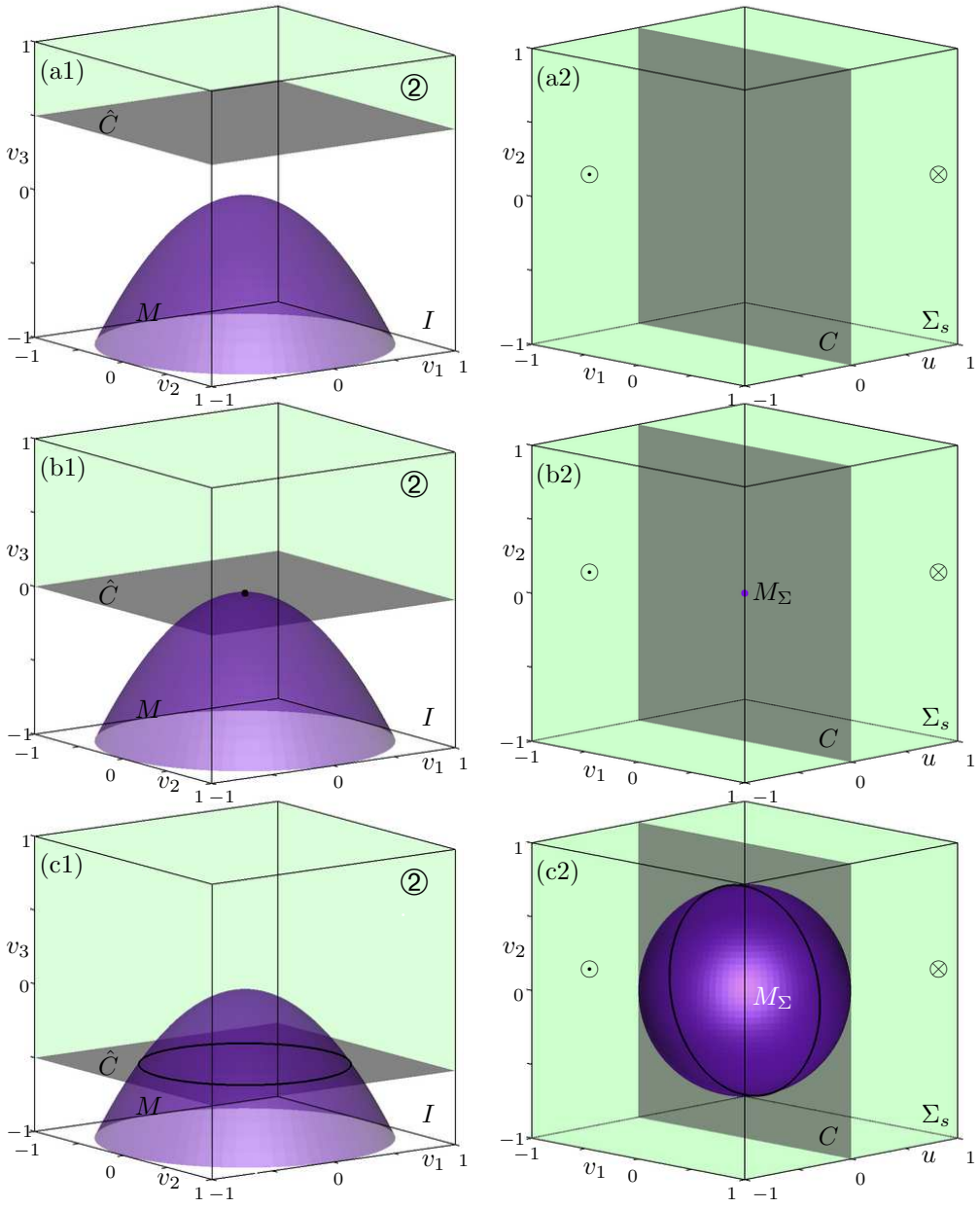

Figure 6. Unfolding of the minimax case of the 2-2-2 tangency bifurcation of a three-dimensional invariant manifold M (purple) with a global section (green); shown are the in-set I (left column) and the section Σ_s (right column); from (a)–(c), $s = 0.5$, $s = 0$, and $s = -0.5$.

Proposition 5. *A 2-2-2 tangency bifurcation of a three-dimensional manifold in* $\mathbb{R}^n$ *is given in the standard flowbox (7) by the family (9) of quadratic sections* Σ_s *with the manifold*

$$M = \{(u, v_1, \ldots, v_{n-1}) \in \mathbb{R}^n \mid v_{n-1} = \pm v_1^2 - v_2^2\,;\ v_i = 0 \text{ for all other } i\,\}. \tag{24}$$

The minus-sign in (24) is referred to as the minimax case and the plus-sign as the saddle case of the 2-2-2 tangency bifurcation. The normal form is given by $n = 4$.

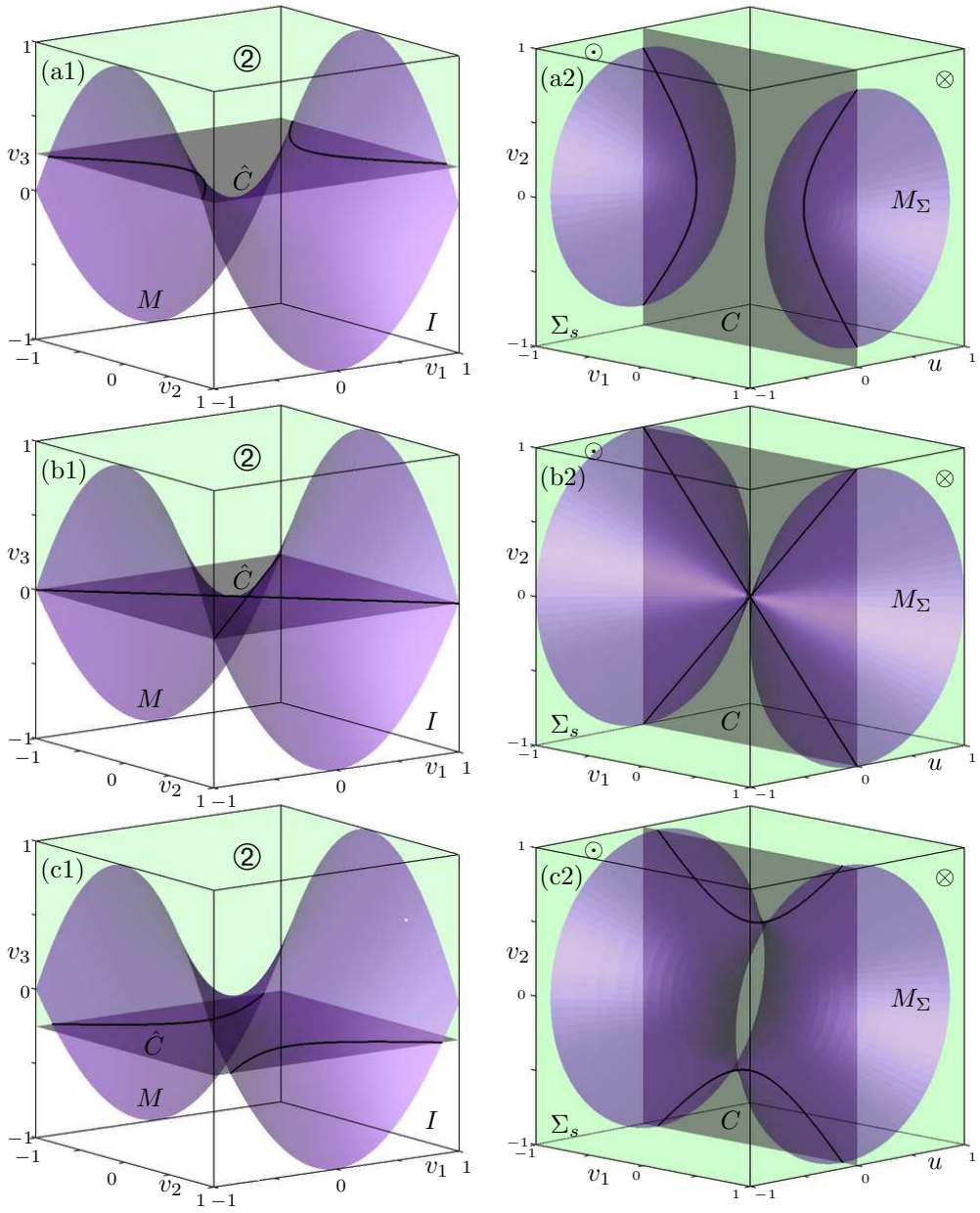

Figure 7. Unfolding of the saddle case of the 2-2-2 tangency bifurcation of a three-dimensional invariant manifold M (purple) with a global section (green); shown are the in-set I (left column) and the section Σ_s (right column); from (a)–(c), $s = 0.5$, $s = 0$, and $s = -0.5$.

The two cases of 2-2-2 tangency bifurcation are shown in figures 6 and 7 before, at and after the bifurcation in terms of the three-dimensional in-set I and the three-dimensional section Σ_s. For any value of the parameter s, the section Σ_s is divided by the critical tangency locus C (the grey plane given by $u = 0$) into two parts with different directions of the flow as indicated. The set $\widehat{C}$ (grey) divides I into two regions: in the green region onto which Σ_s projects, each orbit has two intersections with Σ_s, and in the white region none. The difference between the two cases arises from the fact that

the two-dimensional intersection of the manifold M (purple) in the in-set I is either a maximum or a saddle surface.

For the minimax case in figure 6 the manifold M in the in-set I is a paraboloid with a maximum (or a minimum). There are no intersections between M and Σ_s for positive values of s, so that $M_\Sigma = \emptyset$; see row (a). Decreasing s to the moment of bifurcation at $s = 0$ in row (b), M and Σ_s become tangent at a single point of C; hence, M_Σ now consists of a single point (purple dot) in (b2). As s is decreased further, M_Σ expands into a topological sphere; see row (c). This sphere is bisected by C, and points to the left of C are mapped to points to the right of C. Figure 6 shows that the minimax case of the 2-2-2 tangency bifurcation describes how a compact piece of invariant manifold emerges in or disappears from a three-dimensional Poincaré section.

For the saddle case in figure 7 the manifold in the in-set I is a saddle surface, which intersects $\widehat{C}$ for any value of s. For positive s the saddle point of M in I lies below $\widehat{C}$, which means that M_Σ is composed of two domed surfaces, known as a two-sheeted circular hyperboloid. Each dome is bisected by C and the points on M_Σ to the left of C return on the same dome to the right of C; see (a2). As s decreases the two domes become more pointed until they form a cone at the bifurcation point for $s = 0$; see (b2). The bifurcation arises because the saddle point of M is now contained in $\widehat{C} \subset I$; see (b1). When s is decreased further, as in row (c), the saddle point of M moves into the (green) region of I where points with two intersections with Σ_s originate. Hence, the cone opens up into a one-sheeted hyperboloid; see (c3). Figure 7 shows that the saddle case of the 2-2-2 tangency bifurcation describes how two pieces of invariant manifold in a three-dimensional Poincaré section come together and merge into a single piece.

4.2. The 2-1-2 tangency bifurcation in $\mathbb{R}^4$

We now discuss the situation where there is a quadratic tangency in the direction of the flow, but the intersection of the tangent spaces of M and Σ is of dimension two, rather than three as in section 4.1. As there is a single additional direction of tangency between M and Σ, this tangency is necessarily cubic if the bifurcation is to be of codimension one, meaning that M is given by a cusp surface in the in-set.

Proposition 6. *A 2-1-2 tangency bifurcation of a three-dimensional manifold in* $\mathbb{R}^n$ *is given in the standard flowbox (7) by the family (9) of quadratic sections* Σ_s *with the manifold*

$$M = \{(u, v_1, \ldots, v_{n-1}) \in \mathbb{R}^n \mid v_{n-1} = v_1^3 - v_1 v_2\,;\ v_i = 0 \text{ for all other } i\,\}. \tag{25}$$

The normal form is given by $n = 4$.

The 2-1-2 tangency bifurcation is shown in figure 8 before, at and after the bifurcation in terms of the three-dimensional in-set I and the three-dimensional section Σ_s. As before, Σ_s is divided by C into two parts with different directions of the flow as indicated, while $\widehat{C}$ (grey) divides I into two regions with either two or zero intersections with Σ_s. The manifold M is a cusp surface (purple) that intersects $\widehat{C}$ for any value of

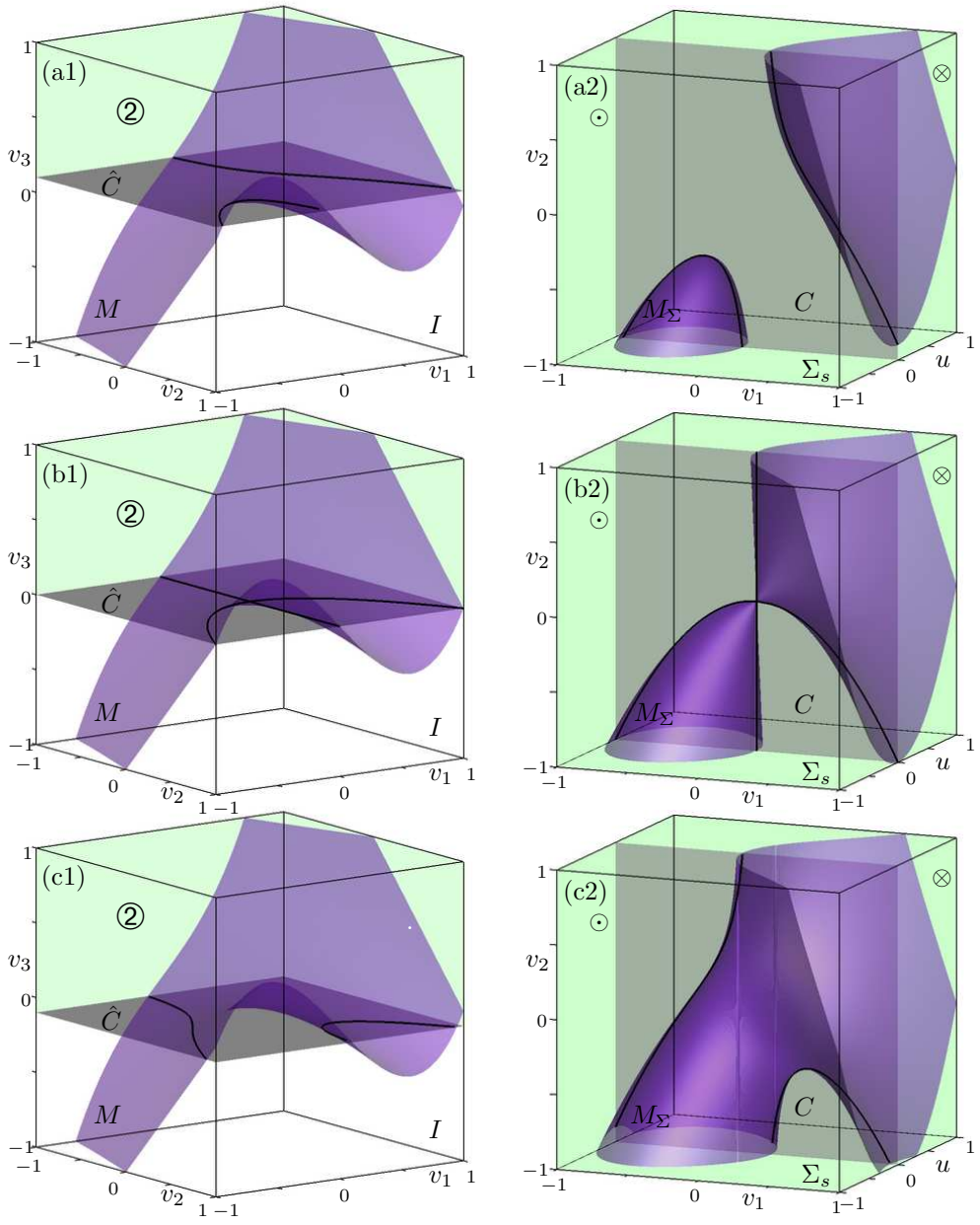

Figure 8. Unfolding of the 2-1-2 tangency bifurcation of a three-dimensional invariant manifold M (purple) with a global section (green); shown are the in-set I (left column) and the section Σ_s (right column); from (a)–(c), $s = 0.1$, $s = 0$, and $s = -0.1$.

the parameter s. For positive s, as in row (a) of figure 8, the cusp point lies in the region of I below $\widehat{C}$ with no intersections, and M_Σ consists of two disjoint parts. At the bifurcation for $s = 0$ in row (b) the cusp point of M lies in $\widehat{C}$, so that the two parts of M_Σ connect at a single point. When s is decreased the cusp point of M lies in the (green) region of I with two intersections with Σ_s, and M_Σ is now a single connected surface.

Figure 8 shows that the 2-1-2 tangency bifurcation provides a different mechanism of how two pieces of invariant manifold in a three-dimensional Poincaré section may merge into a single piece. More specifically, the merging of two pieces of invariant manifold in the Poincaré section does not require that the two tangent spaces of M and Σ_s coincide as is the case for the 2-1-2 tangency bifurcation from section 4.1. The 2-1-2 tangency bifurcation manifests itself in the critical tangency locus C as the unfolding of a pitchfork bifurcation when the normal form symmetry is broken; see, for example, [19]. This is again different from the saddle case of the 2-1-2 tangency bifurcation, which is characterised by a saddle transition in C. The fact that we obtain a pitchfork bifurcation here is due to the invariance of the standard cusp surface M in (25) under the transformation $(v_1, v_2, v_3) \mapsto (-v_1, v_2, -v_3)$, which is a rotation about the v_2-axis over π. When the manifold is deformed away from the normal form the symmetry in the pitchfork may be lost.

4.3. The 3-1-1 tangency bifurcations in $\mathbb{R}^4$

We now consider a tangency bifurcation of a three-dimensional manifold M with an orbit that has a cubic tangency with the section Σ. To obtain a bifurcation of codimension one, there is a single additional direction along which M has a quadratic tangency with Σ. There are two cases that depend on whether the quadratic tangency is away from or towards the critical tangency locus.

Proposition 7. *A 3-1-1 tangency bifurcation of a three-dimensional manifold in* $\mathbb{R}^n$ *is given in the standard flowbox (7) by the family (13) of cubic sections* Σ_s *with the manifold*

$$M = \{(u, v_1, \ldots, v_{n-1}) \in \mathbb{R}^n \mid v_{n-1} = \pm v_2^2 - v_1\,;\ v_i = 0 \text{ for all other } i\,\}. \tag{26}$$

The minus-sign in (24) is referred to as the minimax case and the plus-sign as the saddle case of the 3-1-1 tangency bifurcation. The normal form is given by $n = 4$.

The two cases of 3-1-1 tangency bifurcation are shown in figures 9 and 10 before, at and after the bifurcation in terms of the three-dimensional in-set I, the three-dimensional section Σ_s, and the three-dimensional extended tangency locus $\mathcal{C}$. For any value of the parameter s the section Σ_s is divided by the critical tangency locus C (the grey parabolic cylinder) into two part with different directions of the flow as indicated. The extended tangency locus $\mathcal{C}$ is divided by its critical tangency locus D (the grey plane given by $u = 0$) into two part with different directions of the flow as indicated. The intersection $C = \Sigma \cap \mathcal{C}$ is the cubic green surface given by $v_{n-1} = -u^3 - s$. The set $\widehat{C}$ (grey) consists of two sheets that meet along a curve of cusps (white line). It divides I into two regions, where each orbit has one or three intersections with Σ_s, marked ① and ③ respectively. The difference between the two cases arises from the fact that the manifold M in I either intersects region ③ for all s or there are values of s for which M does not intersect this region.

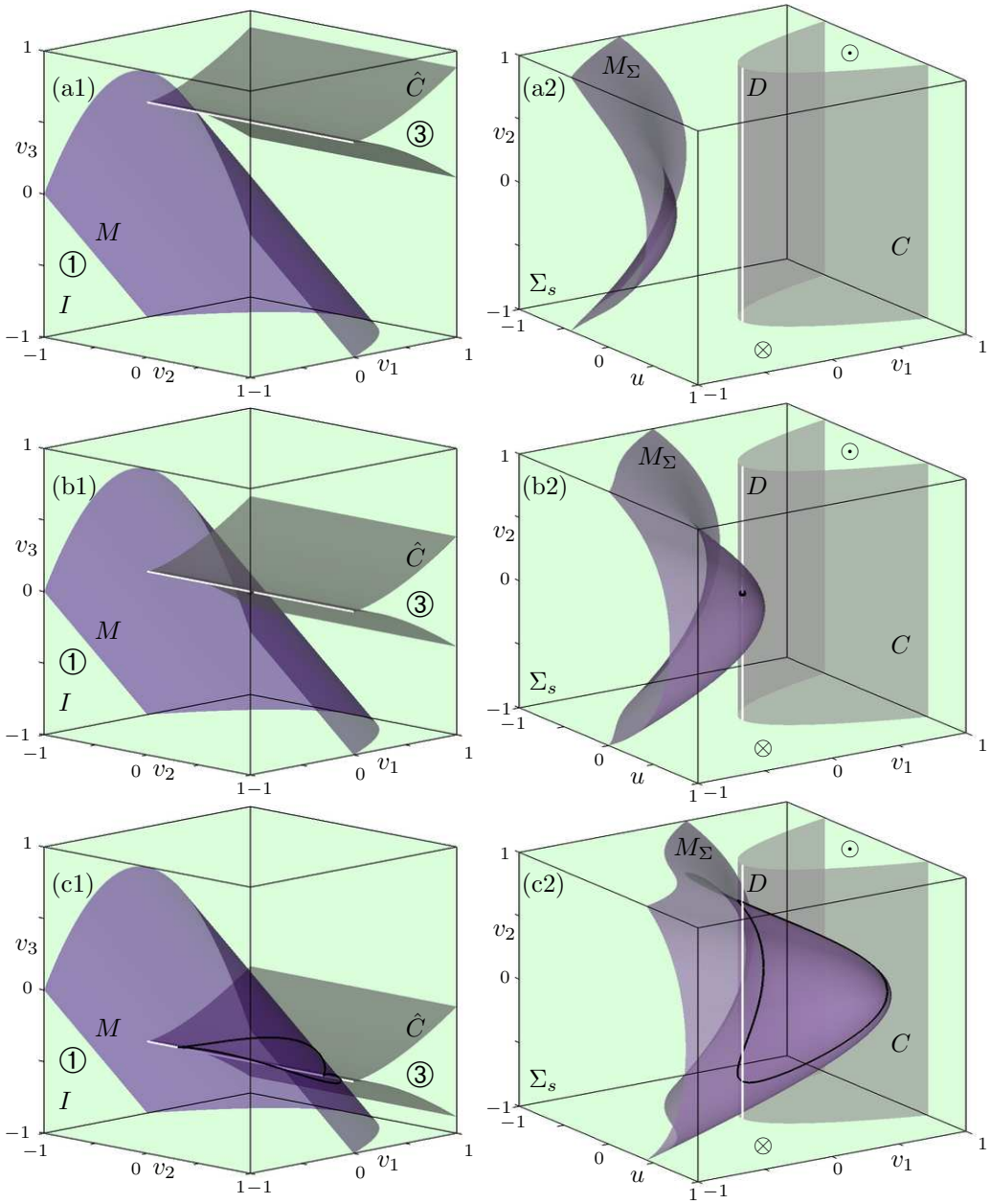

Figure 9. Unfolding of the minimax case of the 3-1-1 tangency bifurcation of a three-dimensional invariant manifold M (purple) with a global section (green); shown are the in-set I (left column) and the section Σ_s (right column); from (a)–(c), $s = 0.5$, $s = 0$, and $s = -0.5$.

For the minimax case in figure 9 the manifold M lies entirely in the region of one intersection with Σ_s when s is positive; see row (a). At the bifurcation point for $s = 0$ in row (b), M touches the cusp line on $\widehat{C}$ in I, meaning that M_Σ becomes tangent to C at a point of its tangency locus D; see (b2). When s is decreased, as in row (c), M intersects $\widehat{C}$ in a closed curve with two cusp points, so that a part of M lies now in region ③; see (c1). As a consequence, M_Σ intersects C in a closed curve; see (c2) and (c3). Figure 9 shows that the minimax case of the 3-1-1 tangency bifurcation describes

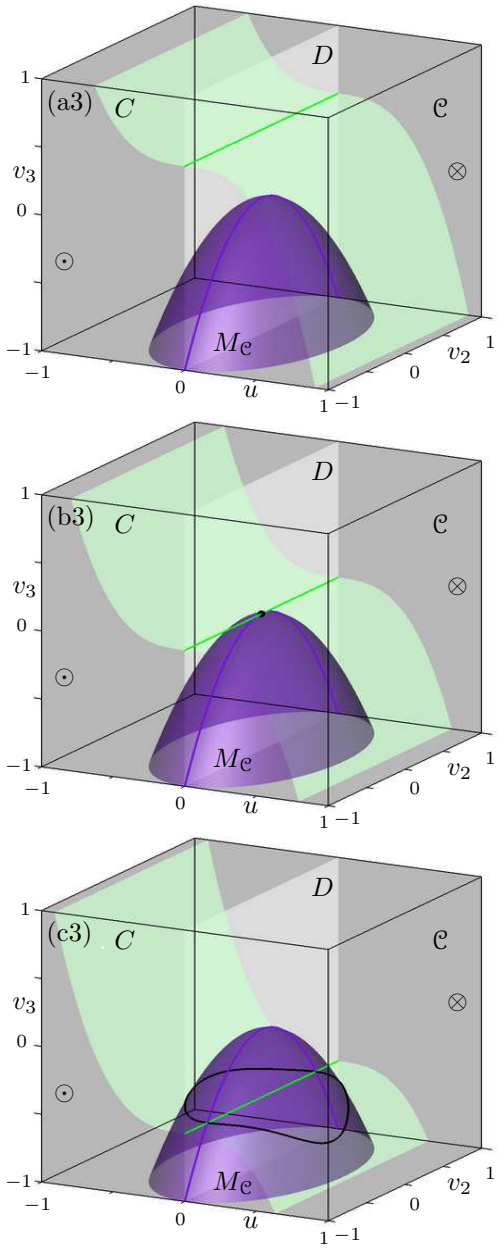

Figure 9. (Continued) Unfolding of the minimax case of the 3-1-1 tangency bifurcation; shown is the extended critical locus $\mathcal{C}$; from (a)–(c), $s = 0.5$, $s = 0$, and $s = -0.5$.

how an invariant manifold of a Poincaré map in a three-dimensional section may develop (or lose) a patch that has two images inside the flowbox under the Poincaré map. Note that this transition manifests itself as a minimax transition between the two surfaces M_Σ and C in Σ_s.

For the saddle case in figure 10 the manifold M always has a part in region ③. For positive s there are two intersection curves of M with $\widehat{C}$, which both cross the cusp line of $\widehat{C}$; see (a1). As a result, there is a part of M_Σ, in between the two curves $M_\Sigma \cap C$, that does not get mapped to another part of M_Σ under the Poincaré map; see (a2) and (a3).

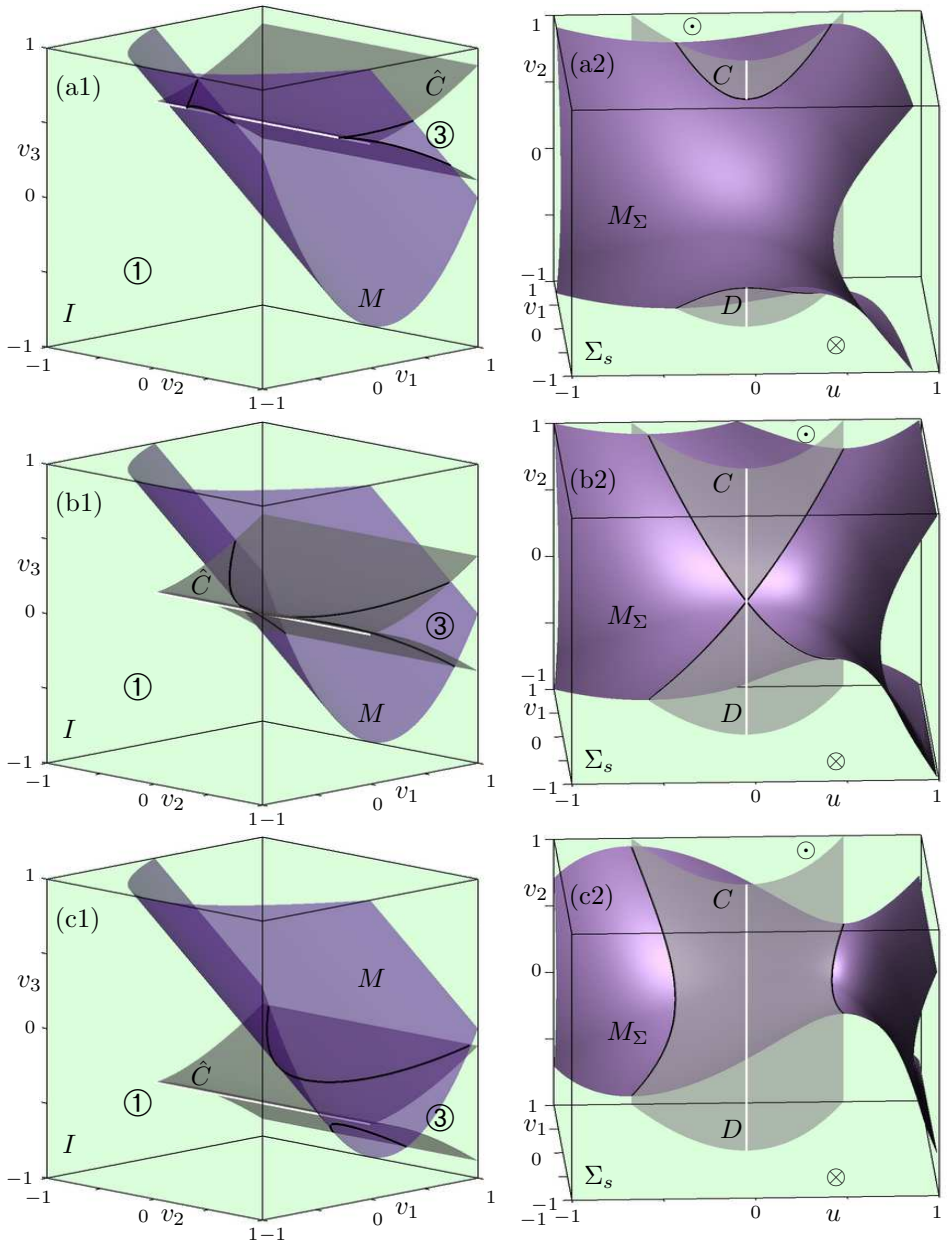

Figure 10. Unfolding of the saddle case of the 3-1-1 tangency bifurcation of a three-dimensional invariant manifold M (purple) with a global section (green); shown are the in-set I (left column) and the section Σ_s (right column); from (a)–(c), $s = 0.5$, $s = 0$, and $s = -0.5$.

At the bifurcation for $s = 0$, as in row (b), the manifold M has a tangency with the cusp line of $\widehat{C}$, which means that the manifold M_Σ becomes tangent to C at a point of D; see (b2) and (b3). After the bifurcation for negative s, as in row (c), there are again two intersection curves of M with $\widehat{C}$, but they now do not cross the cusp line instead they lie entirely in one of the sheets of $\widehat{C}$; see (c1). Therefore, in Σ_s the critical tangency locus C divides the manifold M into three pieces: the left-most piece (for negative u) is mapped to the middle piece (around $u = 0$), which is mapped to the right-most piece

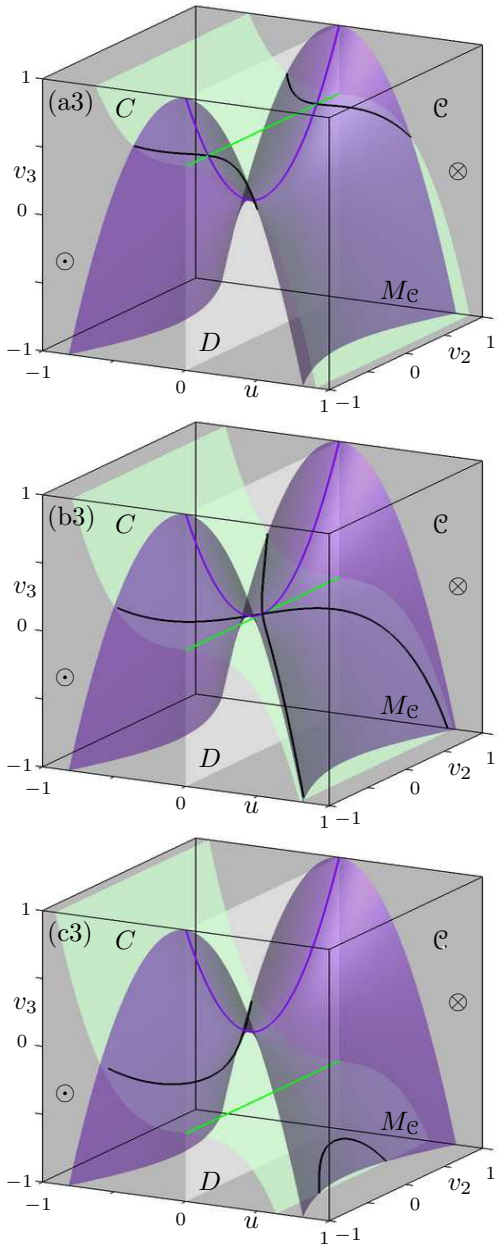

Figure 10. (Continued) Unfolding of the saddle case of the 3-1-1 tangency bifurcation; shown is the extended critical locus $\mathfrak{E}$; from (a)–(c), $s = 0.5$, $s = 0$, and $s = -0.5$.

(for positive u). Figure 10 shows that the saddle case of the 3-1-1 tangency bifurcation describes how an invariant manifold of a Poincaré map in a three-dimensional section may develop (or lose) a patch that has no images inside the flowbox under the Poincaré map. Note that this transition manifests itself as a saddle transition between the two surfaces M_Σ and C in Σ_s.

4.4. The 4-0-0 tangency bifurcation in $\mathbb{R}^4$

The 4-0-0 tangency bifurcation is the first tangency bifurcation with a quartic tangency of an orbit on the manifold M. Such a tangency point may occur generically in $\mathbb{R}^4$ at an isolated point. The section Σ in the flowbox is a swallowtail surface; compare with [1]. For this bifurcation to be of codimension one, we must consider the interaction with a three-dimensional manifold in general position, that is, the tangent spaces of M and Σ only intersect in the direction given by the flow at the tangency point.

Proposition 8. *A 4-0-0 tangency bifurcation of a three-dimensional manifold in* $\mathbb{R}^n$ *is given in the standard flowbox (7) by the family (17) of quartic sections* Σ_s *with the manifold*

$$M = \{(u, v_1, \ldots, v_{n-1}) \in \mathbb{R}^n \mid v_{n-1} = v_1 \,;\; v_i = 0 \text{ for all other } i \,\}. \tag{27}$$

The normal form is given by $n = 4$.

The 4-0-0 tangency bifurcation is shown in figures 11 before, at and after the bifurcation in terms of the three-dimensional in-set I, the three-dimensional section Σ_s, the three-dimensional extended tangency locus $\mathcal{C}$, and the (u, v_3) plane. The latter represents the two-dimensional critical tangency locus D, which is a parabolic cylinder. The set $\widehat{C}$ (grey) in I consist of three sheets that meet along two cusp curves (white), which in turn meet at a swallowtail point. This surface divides I into three regions, where each orbit has zero, two or four intersections with Σ_s, respectively. For any value of the parameter s the section Σ_s is divided into two by the critical tangency locus C (the grey cusp surface) with different directions of flow in each part as indicated. The flow is tangent to C along a fold curve D which has a cusp point at $u = 0$. Similarly, the extended tangency locus $\mathcal{C}$ is divided by its critical tangency locus D (the grey parabolic cylinder) into two parts with different directions of the flow as indicated. The intersection $C = \Sigma \cap \mathcal{C}$ in $\mathcal{C}$ is the quartic green surface given by $v_{n-1} = u^4 - s$.

In figure 11 the manifold M always intersects the surface $\widehat{C}$. For positive s, as in row (a), M intersects the surface $\widehat{C}$ well away from the swallowtail point, so that M_Σ intersects C well way from the cusp point on D. Hence, C divides M_Σ into two pieces; the piece for smaller u is mapped under the Poincaré map to the piece for larger u. Looking at the extended tangency locus $\mathcal{C}$ and its tangency locus this means that $M_\mathcal{C}$ and $C \cap D$ do not intersect. At the bifurcation point the plane M goes exactly through the swallowtail point; see (b1). This means that the manifold M_Σ is tangent to the fold curve D at the cusp point; see (b2). This corresponds to a quadratic tangency of $M_\mathcal{C}$ with C in D; see (b3) and (b4). After the bifurcation for negative s, as in row (c), the plane M intersects all three regions of I. Therefore, in the section Σ_s the set $M_\Sigma \cap C$ crosses the fold curve D on C twice; see (c2). This also means that the curve $M_\mathcal{C}$ in $\mathcal{C}$ now intersects the curve $C = \Sigma \cap D$ at two points; see (c3) and (c4). Figure 11 shows that the 4-0-0 tangency bifurcation describes how an invariant manifold that is mapped to itself once under the Poincaré map in a three-dimensional section may develop (or lose) a patch that has two images inside the flowbox under the Poincaré map. Note that

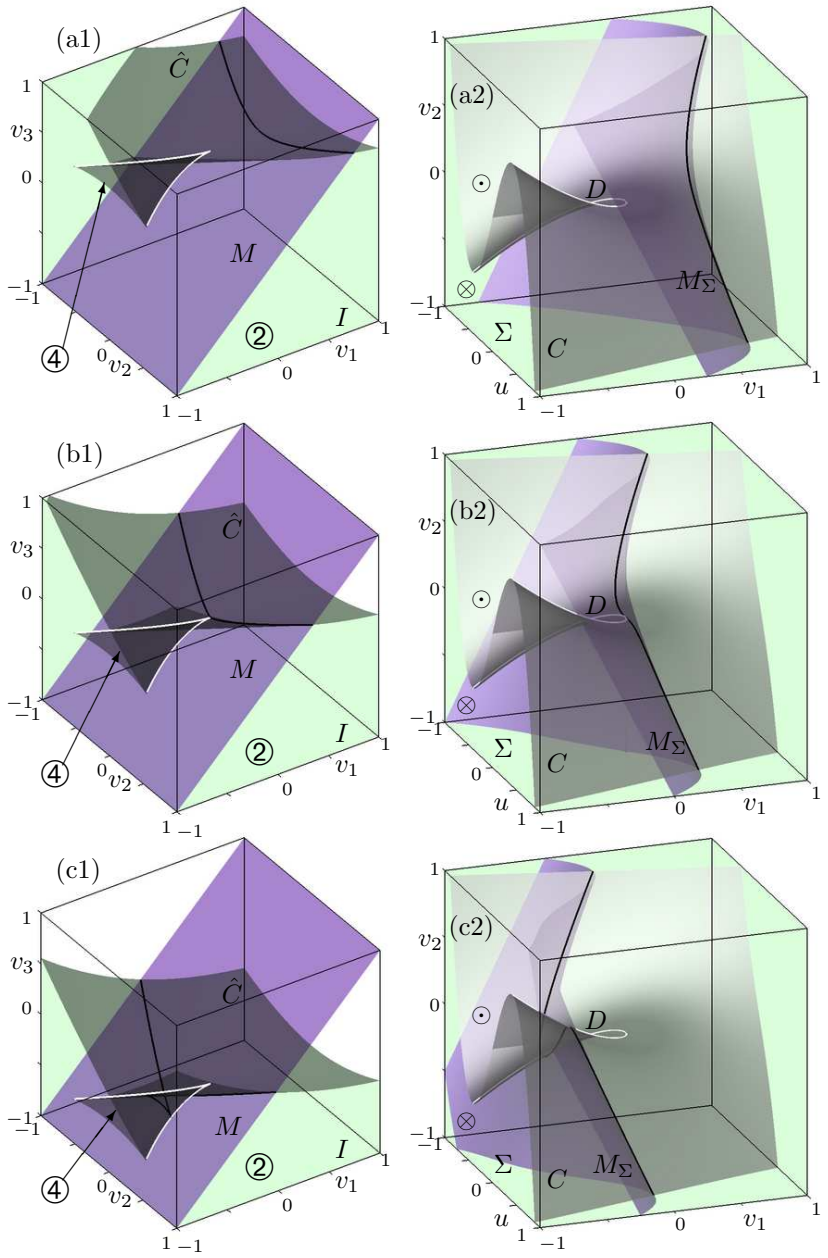

Figure 11. Unfolding of the 4-0-0 tangency bifurcation of a three-dimensional invariant manifold M (purple) with a global section (green); shown are the in-set I (left column) and the section Σ_s (right column); from (a)–(c), $s = 0.5$, $s = 0$, and $s = -0.5$.

this transition manifests itself as a cusp bifurcation between the two surfaces M_Σ and C in Σ_s, which in turn is a quadratic tangency between $M_\mathcal{C}$ and C in the two-dimensional critical tangency locus D of $\mathcal{C}$.

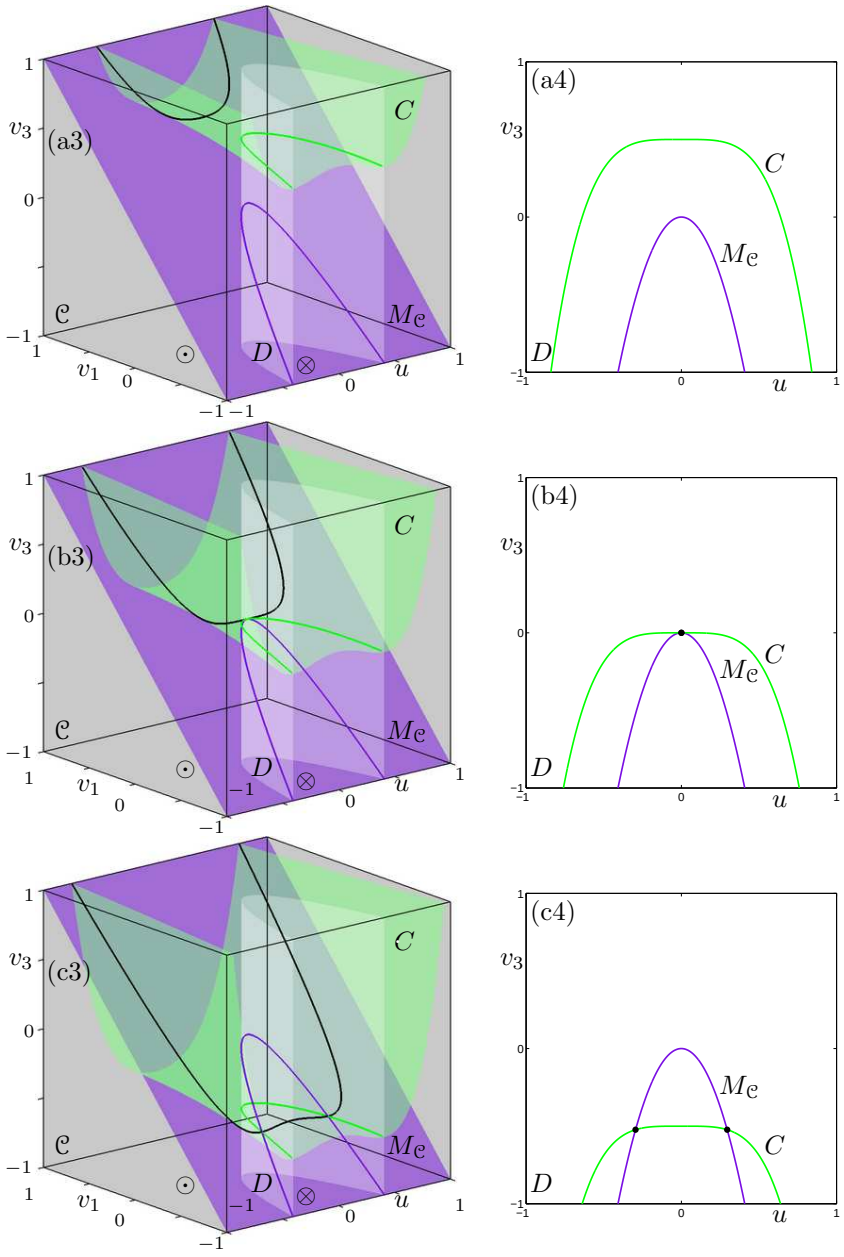

Figure 11. (Continued) Unfolding of the 4-0-0 tangency bifurcation of a three-dimensional invariant manifold M (purple) with a global section (green); shown are the extended critical locus $\mathcal{C}$ (left column) and the intersection of M_Σ with $C = \Sigma \cap D$ in the two-dimensional space D as represented by the (u, v_3)-plane (right column); from (a)–(c), $s = 0.5$, $s = 0$, and $s = -0.5$.

5. Discussion and outlook

We considered tangency bifurcations between an invariant manifold and a Poincaré section in vector fields of dimensions up to four. This type of bifurcation of the associated Poincaré map occurs because the flow becomes tangent to the section. The normal forms for all codimension-one tangency bifurcations were presented within a standard flowbox by a one-parameter family of sections and a fixed invariant manifold. Each

normal form was pictured in the lowest dimension in which it occurs, but the equations were given for any dimension n. It is important to note that the codimension of a tangency bifurcation is independent of the dimension of the vector field. This is so because the dimension $(n-1)$ of the Poincaré section increases with the dimension n of the space, while the manifold remains the same. In our normal forms this means that additional coordinate directions are set to zero, as is stated in the propositions. For example, a quadratic tangency of a one-dimensional manifold with a Poincaré section always gives two intersection points that coalesce before disappearing. Similarly, two-dimensional manifolds always intersect the Poincaré section in curves and three-dimensional manifolds intersect it in surfaces.

We did not present the proofs of genericity of the normal forms here as they each take the following steps. Given a system with a particular tangency type, one identifies a suitable flowbox around the tangency point. Then one maps the intersection of the invariant manifold with the in-set to one of the normal forms, while preserving the flow direction. A second coordinate change that leaves the intersection between the manifold and the in-set invariant (and again preserves the flow direction) can then be constructed to bring the section into its normal form. Explicit proofs for the tangency bifurcations in two- and three-dimensional vector fields are given in [10]; see also [18, 20, 16, 21, 11]

Tangency bifurcations of codimension greater than one can be studied in the same way, but then more unfolding parameters are needed to fully investigate the bifurcation. Note that there is always the problem of finding a way in which to display all the information in dimensions larger than three. Our approach here was to illustrate four-dimensional flows in a flowbox by presenting different projections onto suitable sides of the box. This technique is right at the boundary of what can be achieved for four-dimensional flows.

Now that we have classified them, the next step is to consider how tangency bifurcations affect the Poincaré return map in a given vector field arising in an application. The case of a quadratic tangency of a one-dimensional attracting periodic orbit with a two-dimensional section was treated in [10]. Depending on the choice of section there are either areas where the Poincaré map is undefined or there are points of discontinuity of the map. This one-dimensional quadratic tangency will have the same effect on the global dynamics also in higher dimensions. In ongoing work we are studying the possible dynamical consequences of the other tangency bifurcations of invariant manifolds — initially for two-dimensional Poincaré sections.

Acknowledgements

The authors thank David Chillingworth for fruitful discussions and Mike R Jeffrey for his valuable comments on a draft of this paper. The research of HMO was supported by an Advanced Research Fellowship grant from the Engineering and Physical Sciences Research Council (EPSRC).

[1] V. I. Arnol′d. *Catastrophe Theory*. Springer-Verlag, 3rd edition, 1992.

[2] G. D. Birkhoff. Dynamical systems with two degrees of freedom. *Trans. Am. Math. Soc.*, 18(2):199–300, 1917.

[3] P. Collins and B. Krauskopf. Entropy and bifurcations in a chaotic laser. *Phys. Rev. E*, 66(5):056201, 2002.

[4] J. P. England, B. Krauskopf, and H. M. Osinga. Computing one-dimensional global manifolds of Poincaré maps by continuation. *SIAM J. App. Dyn. Sys.*, 4(4):1008–1041, 2005.

[5] M. Golubitsky and D. G. Schaeffer. *Singularities and Groups in Bifurcation Theory*, volume 1. Springer-Verlag, 1985.

[6] K. Green and B. Krauskopf. Global bifurcations and bistability at the locking boundaries of a semiconductor laser with phase-conjugate feedback. *Phys. Rev. E*, 66(1):016220, 2002.

[7] J. Guckenheimer and P. Holmes. *Nonlinear Oscillations, Dynamical Systems, and Bifurcations of Vector Fields*. Springer-Verlag, 1983.

[8] W. Just and H. Kantz. Some considerations on Poincaré maps for chaotic flows. *J. Phys. A: Math. Gen.*, 33:163–170, 2000.

[9] Y. A. Kuznetsov. *Elements of Applied Bifurcation Theory*. Springer-Verlag, 2004.

[10] C. M. Lee, P. J. Collins, B. Krauskopf, and H. M. Osinga. Tangency bifurcations of global Poincaré maps. *SIAM J. App. Dyn. Sys.*, 7(3):712–754, 2008.

[11] S. Mancini, M. A. S. Ruas, and M. A. Teixeira. On divergent diagrams of finite codimnsion. *Portugaliae Mathematica, Nova Série*, 50(2):179–194, 2002.

[12] F. B. Marten, S. Rodrigues, O. J. Benjamin, M. P. Richardson, and J. R. Terry. Onset of polyspike complexes in a mean-field model of human eeg and its application to absence epilepsy. *Phil. Trans. Royal Soc.*, A in press, 2008.

[13] J. Palis and W. de Melo. *Geometric Theory of Dynamical Systems*. Springer-Verlag, 1982.

[14] R. Peikert and F. Sadlo. *Eurographics/IEEE-VGTC Symposium on Visualization*, chapter Visualization methods for vortex rigs and vortex breakdoen bubbles. The Eurographics Association, 2007.

[15] R. Peikert and F. Sadlo. *Topology-based Methods in Visualization*, chapter Flow topology beyond skeletons: visualization of features in recirculating flow. Springer-Verlag, 2007.

[16] P. B. Percell. Structural stability on manifolds with boundary. *Topology*, (12):123–144, 1973.

[17] T. Poston and I. Stewart. *Catastrophy Theory and its Applications*. Pitman Publishing Ltd., 1978.

[18] J. Sotomayor and M. A. Teixeira. *Dynamical Systems Valparaiso 1986*, volume 1331 of *Lecture Notes in Mathematics*, chapter Vector fields near the boundary of a 3–manifold, pages 169–195. Springer–Verlag, 1988.

[19] S. H. Strogatz. *Nonlinear Dynamics and Chaos: With applications to Physics, Biology, Chemistry, and Engineering*. Addison-Wesley, 1994.

[20] M. A. Teixeira. Generic bifurcation in manifolds with boundary. *J. Diff. Equ.*, 25(1):65–89, 1977.

[21] M. A. Teixeira. Generic bifurcatins of sliding vector fields. *J. Math. Anal. Appl.*, (176):436–457, 1993.

[22] X.-S. Yang. A remark on global Poincaré section and suspension manifold. *Chaos, Solitons and Fractals*, 11:2157–2159, 2000.